Control of Hsp90 chaperone and its clients by N-terminal acetylation and the N-end rule pathway

Jang-Hyun Oh[a], Ju-Yeon Hyun[a], and Alexander Varshavsky[a,1]

[a]Division of Biology and Biological Engineering, California Institute of Technology, Pasadena, CA 91125

Contributed by Alexander Varshavsky, April 18, 2017 (sent for review April 10, 2017; reviewed by Avram Hershko and William P. Tansey)

We found that the heat shock protein 90 (Hsp90) chaperone system of the yeast *Saccharomyces cerevisiae* is greatly impaired in *naa10Δ* cells, which lack the NatA N^{α}-terminal acetylase (Nt-acetylase) and therefore cannot N-terminally acetylate a majority of normally N-terminally acetylated proteins, including Hsp90 and most of its cochaperones. Chk1, a mitotic checkpoint kinase and a client of Hsp90, was degraded relatively slowly in wild-type cells but was rapidly destroyed in *naa10Δ* cells by the Arg/N-end rule pathway, which recognized a C terminus-proximal degron of Chk1. Diverse proteins (in addition to Chk1) that are shown here to be targeted for degradation by the Arg/N-end rule pathway in *naa10Δ* cells include Kar4, Tup1, Gpd1, Ste11, and also, remarkably, the main Hsp90 chaperone (Hsc82) itself. Protection of Chk1 by Hsp90 could be overridden not only by ablation of the NatA Nt-acetylase but also by overexpression of the Arg/N-end rule pathway in wild-type cells. Split ubiquitin-binding assays detected interactions between Hsp90 and Chk1 in wild-type cells but not in *naa10Δ* cells. These and related results revealed a major role of Nt-acetylation in the Hsp90-mediated protein homeostasis, a strong up-regulation of the Arg/N-end rule pathway in the absence of NatA, and showed that a number of Hsp90 clients are previously unknown substrates of the Arg/N-end rule pathway.

Naa10 | Chk1 | Ubr1 | Ufd4 | protein degradation

Proteins called chaperones promote the in vivo protein folding and counteract misfolding, maladaptive protein aggregation, and other perturbations of proteostasis (1–4). Hsp90 is an ATP-dependent chaperone system that mediates the conformational maturation and stabilization of many proteins. Referred to as Hsp90 clients, these proteins include kinases, transcriptional regulators, and many other proteins that comprise at least 20% of a cellular proteome. The diversity of Hsp90 clients and the broad range of processes that involve Hsp90 underlie its necessity for cell viability in all eukaryotes (5–11). Cochaperones of the ∼90-kDa Hsp90 comprise, in mammals, ∼30 distinct proteins. They participate in the delivery of clients to Hsp90 and contribute to related processes, including ATP hydrolysis by Hsp90 (12). Because of its ability to modulate protein conformations, the Hsp90 system can either exacerbate or counteract the fitness-reducing effects of mutations in cellular proteins. This property of Hsp90 affects the standing genetic variation and thereby influences the impact of natural selection on rates and directions of evolution (13, 14).

The N-end rule pathways comprise a set of proteolytic systems whose unifying feature is their ability to recognize proteins containing N-terminal (Nt) degradation signals called N-degrons, thereby causing the degradation of these proteins by the proteasome or autophagy in eukaryotes and by the proteasome-like ClpAP protease in bacteria (Fig. 1) (15–26). The main determinant of an N-degron is a destabilizing Nt-residue of a protein. Many N-degrons become active through their enzymatic Nt-acetylation, Nt-formylation, Nt-deamidation, Nt-arginylation, or Nt-leucylation. Studies over the last three decades have shown that all 20 amino acids of the genetic code can act, in cognate sequence contexts, as destabilizing Nt-residues. Consequently, many, possibly most, proteins in a cell are conditionally short-lived N-end rule substrates, either as full-length proteins or as protease-generated natural protein fragments (21, 27). Recognition components of N-end rule pathways are called "N-recognins." In eukaryotes, N-recognins are E3 ubiquitin (Ub) ligases that can target N-degrons (Fig. 1).

Regulated degradation of proteins or their fragments by N-end rule pathways has been shown to mediate a wide range of processes, including the sensing of oxygen, nitric oxide (NO), heme, and short peptides; the control of subunit stoichiometry in protein complexes; the elimination of misfolded proteins; the degradation of proteins retrotranslocated to the cytosol from other compartments; the regulation of apoptosis and repression of neurodegeneration; the regulation of DNA repair, transcription, replication, and chromosome cohesion/segregation; the regulation of G proteins, cytoskeletal proteins, autophagy, gluconeogenesis, peptide import, meiosis, immunity, circadian rhythms, fat metabolism, cell migration, cardiovascular development, spermatogenesis, and neurogenesis; the functioning of organs, including the brain, muscle, testis, and pancreas; and the regulation of leaf and shoot development, oxygen/NO sensing, and many other processes in plants (refs. 15–17, 21–24, 28, and the references therein).

Eukaryotes contain three N-end rule pathways. One of them, the Arg/N-end rule pathway, targets unacetylated Nt-residues (Fig. 1*B*) (18, 29–31). N-terminal Arg, Lys, His, Leu, Phe, Tyr, Trp, Ile, and Met (if Met is followed by a bulky hydrophobic residue) are directly recognized by N-recognins (15, 27, 32). In contrast, N-terminal Asn, Gln, Glu, and Asp (as well as Cys, under some conditions) are destabilizing because of the enzymatic deamidation of N-terminal Asn and Gln and the arginylation of N-terminal Asp, Glu, and (oxidized) Cys (33–37).

In the yeast *Saccharomyces cerevisiae*, the Arg/N-end rule pathway is mediated by the Ubr1 N-recognin, a 225-kDa RING-type E3 Ub ligase and a part of the targeting complex comprising the Ubr1–Rad6 and Ufd4–Ubc4/5 E3-E2 holoenzymes (Fig. 1*B*) (38).

Significance

We found that the yeast Hsp90 chaperone system is greatly impaired in *naa10Δ* cells, which cannot N-terminally acetylate a majority of normally N-terminally acetylated proteins, including Hsp90 and its cochaperones. Hsp90 clients, including Chk1, Kar4, Tup1, Gpd1, Ste11, and even the Hsp90 chaperone (Hsc82) itself, became short-lived substrates of the Arg/N-end rule pathway in *naa10Δ* cells. Ubr1 targets the Chk1 kinase through its internal degron. Interactions of Hsp90 with Chk1 could be detected in wild-type but not in *naa10Δ* cells. These results revealed a major role of N-terminal acetylation in the Hsp90-mediated protein homeostasis and showed that a number of Hsp90 clients are previously unknown substrates of the Arg/N-end rule pathway.

Author contributions: J.-H.O. and A.V. designed research; J.-H.O. and J.-Y.H. performed research; J.-H.O., J.-Y.H., and A.V. analyzed data; and J.-H.O. and A.V. wrote the paper.

Reviewers: A.H., Technion Israel Institute of Technology; and W.P.T., Vanderbilt University School of Medicine.

The authors declare no conflict of interest.

[1]To whom correspondence should be addressed. Email: avarsh@caltech.edu.

This article contains supporting information online at www.pnas.org/lookup/suppl/doi:10.1073/pnas.1705898114/-/DCSupplemental.

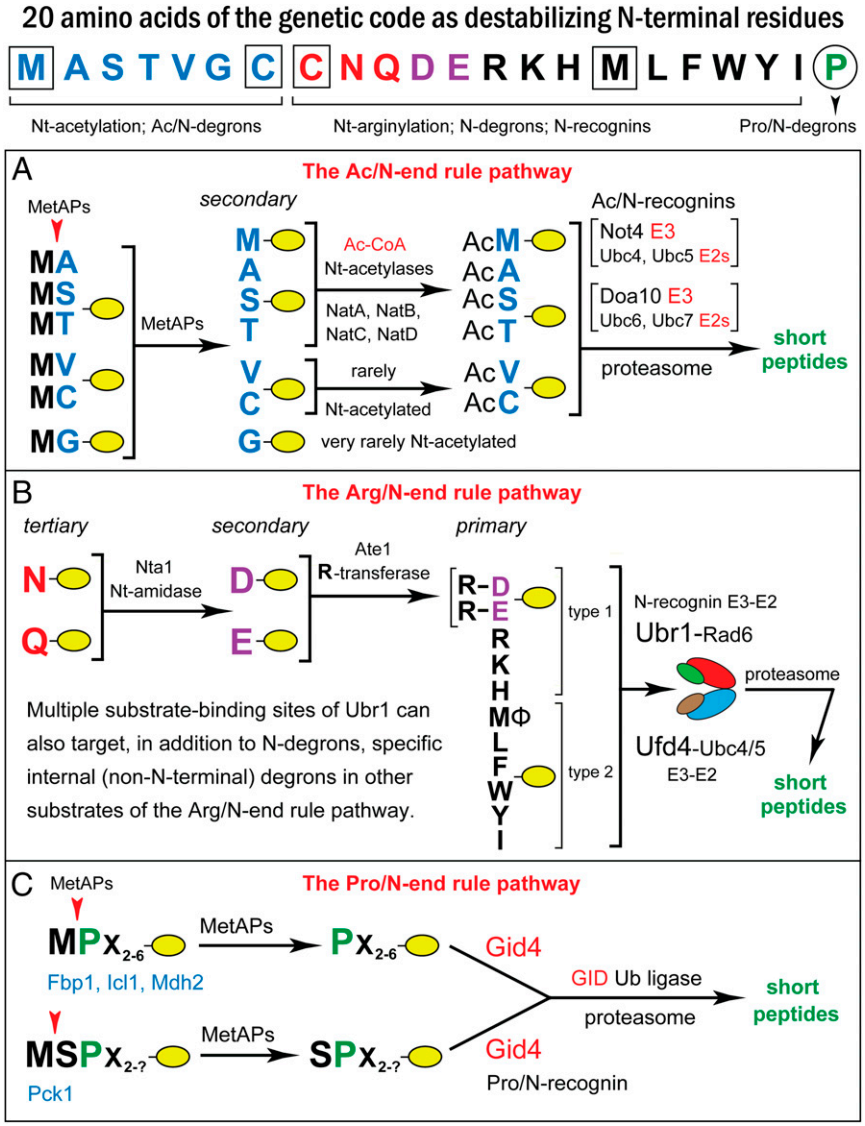

Fig. 1. The N-end rule pathways. N-terminal residues at the top of the diagram are indicated by single-letter abbreviations. Twenty DNA-encoded amino acids are arranged to delineate three sets of N-degrons in *S. cerevisiae*, corresponding to three N-end rule pathways. N-terminal Met is cited twice, because it can be recognized by the Ac/N-end rule pathway (as Nt-acetylated N-terminal Met) and by the Arg/N-end rule pathway (as unacetylated N-terminal Met). N-terminal Cys is also cited twice, because it can be recognized by the Ac/N-end rule pathway (as Nt-acetylated Cys) and by the Arg/N-end rule pathway (as an oxidized, Nt-arginylatable N-terminal Cys, denoted as Cys* and formed in multicellular eukaryotes but apparently not in unstressed *S. cerevisiae*). (*A*) The Ac/N-end Rule pathway. (*B*) The Arg/N-end rule pathway. (*C*) The Pro/N-end rule pathway. See the Introduction for references and brief descriptions of these pathways.

Two substrate-binding sites of Ubr1 recognize N-degrons, whereas its other binding sites recognize internal degrons in proteins such as Cup9 or a variety of misfolded proteins (39–43). Thus, physiological substrates of the Arg/N-end rule pathway comprise not only proteins bearing N-degrons but also proteins containing internal degrons.

Another N-end rule pathway is the Ac/N-end rule pathway. It recognizes N^{α}-terminally acetylated (Nt-acetylated) residues (Fig. 1*A*) (20, 27, 28, 44). N-degrons and E3 Ub ligases of the Ac/N-end rule pathway are called Ac/N-degrons and Ac/N-recognins, respectively. At least 60% of *S. cerevisiae* proteins and ∼90% of human proteins are cotranslationally and irreversibly Nt-acetylated by ribosome-associated Nt-acetylases (Fig. 1*A*) (45, 46). In examined cases, the presence of the Nt-Ac group in a subunit of a protein complex increases the thermodynamic stability of the complex, because affinity-enhancing contacts by the Nt-Ac group cause a slower dissociation of the Nt-acetylated subunit (as compared with its unacetylated counterpart) from the rest of the complex (47–50). Many, possibly most, Nt-acetylated proteins contain Ac/N-degrons, whose regulation includes their steric shielding in cognate protein complexes (44).

The third eukaryotic N-end rule pathway, the Pro/N-end rule pathway, is mediated by the GID Ub ligase. Gid4, a subunit of GID that functions as the Pro/N-recognin, targets proteins that bear the N-terminal Pro residue or a Pro at position 2, in addition to adjoining (and also required) sequence motifs (Fig. 1*C*) (21). Physiological substrates of the Pro/N-end rule pathway include gluconeogenic enzymes, which are long-lived in cells deprived of glucose but are selectively destroyed upon return to glucose-replete conditions (21, 51, 52).

We show here that the yeast Hsp90 chaperone system is greatly impaired in *naa10Δ* cells, which lack the NatA Nt-acetylase and therefore cannot Nt-acetylate a majority of normally Nt-acetylated proteins. By exploring this finding, we identified extensive connections between Hsp90 and the Arg/N-end rule pathway. These and related results revealed a major role of Nt-acetylation in the Hsp90-mediated protein homeostasis, a strong up-regulation of the Arg/N-end rule pathway in the absence of NatA, and also showed that a number of Hsp90 clients are previously unknown substrates of the Arg/N-end rule pathway.

Results

Promoter Reference Technique. Degradation assays used the promoter reference technique (PRT) (Fig. 2 *A* and *B*) (21). In this method, one measures, during a chase, the ratio of a test protein to a long-lived reference protein, the mouse dihydrofolate reductase (DHFR). The reference protein and test proteins were

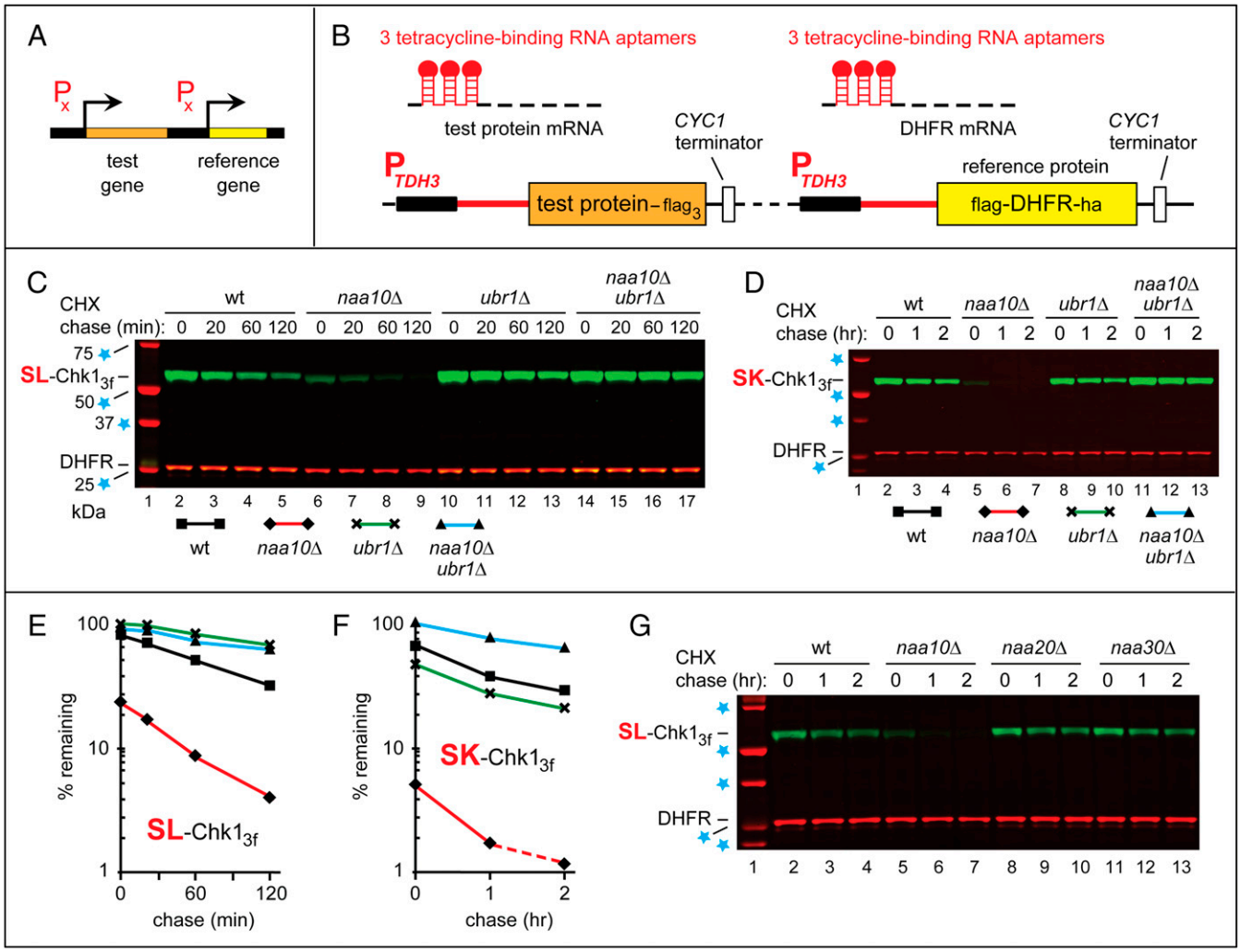

Fig. 2. The PRT and degradation of Chk1 in *naa10Δ* cells. (*A* and *B*) The PRT. See the main text for a discussion. (*C*) Lane 1, kDa markers. CHX-chases, using PRT with wild-type SL-Chk1$_{3f}$, were performed at 30 °C for 0, 20, 60, and 120 min, with wild-type (lanes 2–5), *naa10Δ* (lanes 6–9), *ubr1Δ* (lanes 10–13), and *naa10Δ ubr1Δ* (lanes 14–17) *S. cerevisiae*. Extracts were prepared from cells withdrawn at the indicated times of a chase. Proteins in an extract were fractionated by SDS/PAGE, followed by immunoblotting with anti-flag and anti-HA antibodies. (*D*) As in *C*, but CHX-chases, with the SK-Chk1$_{3f}$ mutant, were for 0, 1, and 2 h, with wild-type (lanes 2–4), *naa10Δ* (lanes 5–7), *ubr1Δ* (lanes 8–10), and *naa10Δ ubr1Δ* (lanes 11–13) *S. cerevisiae*. (*E* and *F*) Quantification of data in *C* and *D*, respectively. For curve designations, see the keys below the immunoblots in *C* and *D*. All degradation assays in this study were performed at least twice, yielding results that differed by less than 10%. (*G*) As in *C*, but CHX-chases, with wild-type SL-Chk1$_{3f}$, were for 0, 1, and 2 h, with wild-type (lanes 2–4), *naa10Δ* (lanes 5–7), *naa20Δ* (lanes 8–10), and *naa30Δ* (lanes 11–13) *S. cerevisiae*. In *C*, *D*, and *G*, lane 1 shows kDa markers and blue stars denote 25-, 37-, 50-, and 75-kDa proteins.

coexpressed on a low-copy plasmid from two identical P_{TDH3} promoters containing additional DNA elements developed by others (53). Once transcribed into an mRNA, these elements form 5′-RNA aptamers that can bind to tetracycline (Tc), thereby repressing translation of that mRNA in *cis* (Fig. 2*B*). This PRT design improves degradation assays in two independent ways: by providing a reference protein and by allowing chases that involve a gene-specific (Tc-mediated) repression of translation.

Chk1 Kinase Is Short-Lived in *naa10Δ* Cells. This work began with a finding about the *S. cerevisiae* mitotic checkpoint kinase Chk1 (SL-Chk1, bearing N-terminal Ser-Leu) (54). C-terminally flag-tagged wild-type SL-Chk1$_{3f}$ was relatively long-lived in wild-type cells but became short-lived in *naa10Δ* (*ard1Δ*) cells, which lacked the NatA Nt-acetylase (Fig. 2 *C* and *E* and *SI Appendix*, Fig. S2 *A*, *C*, and *D*).

The accelerated degradation of SL-Chk1$_{3f}$ in *naa10Δ* cells was manifested, in part, by much lower prechase (time-zero) levels of SL-Chk1$_{3f}$ in these cells (Fig. 2 *C* and *E* and *SI Appendix*, Fig. S2 *A*, *C*, and *D*). ^{35}S-pulse-chases with SL-Chk1$_{3f}$ produced similar results (*SI Appendix*, Fig. S2*B*). We could ascribe the decreased prechase levels of SL-Chk1$_{3f}$ in *naa10Δ* cells to its faster degradation (rather than to a decreased synthesis of Chk1), inasmuch as these assays used PRT and its built-in reference protein (Fig. 2*B*). As shown earlier, prechase effects analogous to those in *naa10Δ* vs. wild-type cells stem from the accelerated destruction of nascent and/or newly formed proteins (15, 27, 44). This aspect of SL-Chk1$_{3f}$ degradation was particularly prominent in *naa10Δ* cells (Fig. 2 *C* and *E* and *SI Appendix*, Fig. S2 *A*, *C*, and *D*).

The faster degradation of SL-Chk1$_{3f}$ in *naa10Δ* cells was NatA-specific: This effect was absent in *naa20Δ* cells (which lacked the NatB Nt-acetylase) and in *naa30Δ* cells (which lacked the NatC Nt-acetylase) (Fig. 2*G*). An ectopic expression of NatA (Naa10) in *naa10Δ* cells (monitored by antibody to Naa10) restored the relative stability of SL-Chk1$_{3f}$ (Fig. 3*A*).

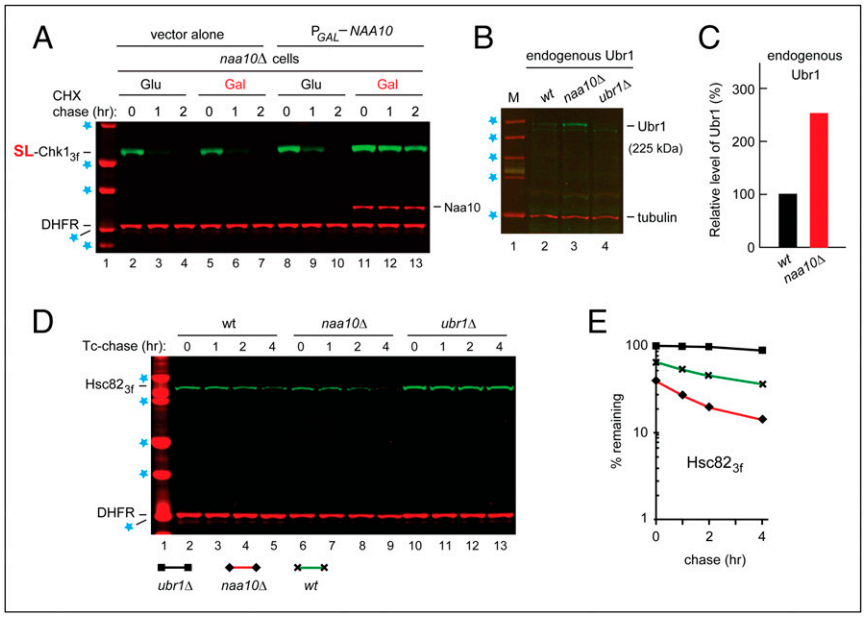

Fig. 3. Degradation of Hsc82 by the Arg/N-end rule pathway in *naa10Δ* cells. (*A*) CHX-chases, using PRT (Fig. 2*B*), with wild-type SL-Chk1$_{3f}$, for 0, 1, and 2 h, with *naa10Δ S. cerevisiae* carrying a high-copy plasmid that expressed Naa10 from the P_{GAL} promoter. Lane 1, kDa markers. Blue stars denote 20-, 25-, 37-, 50-, and 75-kDa markers, respectively. Lanes 2–4 and 5–7, cells (containing vector alone) in glucose and galactose medium, respectively. Lanes 8–10 and 11–13 are as in lanes 2–4 and 5–7, respectively, but with cells containing the *P_{GAL}-NAA10* plasmid. The presence of Naa10 was verified directly, using an affinity-purified antibody to Naa10 (bands in lanes 11–13, above the bands of DHFR). (*B*) Immunoblotting-based comparison of the levels of endogenous (untagged) Ubr1 in wild-type *naa10Δ* and *ubr1Δ S. cerevisiae* (with *ubr1Δ* cells as a negative control), using an affinity-purified antibody to Ubr1 (see the main text), with immunoblots of tubulin as a loading control. Blue stars denote 50-, 75-, 100-, 150-, and 250-kDa markers, respectively. (*C*) Quantification of the data in *B*, with subtraction of the background-level signal in lane 4 (*ubr1Δ* cells) and with the level of Ubr1 in wild-type cells taken as 100%. (*D*) Degradation of Hsc82 in *naa10Δ* cells. Blue stars denote 25-, 37-, 50-, 75-, and 100-kDa markers, respectively. Tc-chases, using PRT (Fig. 2*B*) with wild-type Hsc82$_{3f}$, were for 0, 1, 2, and 4 h, with wild-type (lanes 2–5), *naa10Δ* (lanes 6–9), and *ubr1Δ* (lanes 10–13) *S. cerevisiae*. Extracts were prepared from cells withdrawn at the indicated times of a chase. Proteins in an extract were fractionated by SDS/PAGE, followed by immunoblotting with anti-flag and anti-HA antibodies. (*E*) Quantification of data in *D*. For curve designations, see the keys below the immunoblot in *D*. All chases in this study were performed at least twice, yielding results that differed by less than 10%.

Chk1 as a Substrate of the Arg/N-End Rule Pathway in *naa10Δ* Cells. The E3 Ub ligases Ubr1 and Ufd4 are a part of the targeting apparatus of the Arg/N-end rule pathway (Fig. 1*B*). Remarkably, the ablation of either Ubr1 or Ufd4 abrogated the accelerated degradation of SL-Chk1$_{3f}$ in *naa10Δ* cells. SL-Chk1$_{3f}$ was as stable in *ubr1Δ naa10Δ* and *ufd4Δ naa10Δ* double mutants as it was in wild-type cells, despite the absence of the NatA (Naa10) Nt-acetylase in double mutants and in contrast to the rapid degradation of SL-Chk1$_{3f}$ in single-mutant *naa10Δ* cells (Figs. 2 *C* and *E* and *SI Appendix*, Fig. S2 *A*, *C*, and *D*). As would be expected (Fig. 1*B*), the degradation of SL-Chk1$_{3f}$ required the proteasome (Fig. 4*D*).

Degradation of Chk1 in *naa10Δ* Cells Does Not Involve the Cup9 Regulon. Cup9, a transcriptional repressor of a regulon containing ∼50 genes, is conditionally destroyed by the Arg/N-end rule pathway through an internal degron of Cup9 (39). It was conceivable that the tripartite Cup9–Tup1–Ssn6 repressor complex (39) might dissociate more rapidly in the absence of NatA-mediated Nt-acetylation, because of the "affinity" effect of Nt-Ac groups (described in the Introduction). This effect would lead to a faster degradation of Cup9 by the Arg/N-end rule pathway in *naa10Δ* cells and, consequently, to an induction of the Cup9 regulon, whose functions are incompletely understood. We therefore asked whether the faster degradation of SL-Chk1$_{3f}$ in *naa10Δ* cells might be mediated by the Arg/N-end rule pathway indirectly, through a faster destruction of Cup9 and the resulting up-regulation of a member of the Cup9 regulon (e.g., an uncharacterized Ub ligase) that would accelerate the degradation of SL-Chk1$_{3f}$ in *naa10Δ* cells. This model was found to be incorrect, inasmuch as SL-Chk1$_{3f}$ remained relatively long-lived in *cup9Δ* cells, in which the Cup9 regulon becomes derepressed (Fig. 4*E*) (39).

Endogenous Chk1 and Its Targeting by the Arg/N-End Rule Pathway. To address the degradation of endogenous SL-Chk1, we replaced the chromosomal *CHK1* gene with a DNA segment that expressed wild-type SL-Chk1 C-terminally tagged with myc (SL-Chk1$_{9m}$) from the endogenous P_{CHK1} promoter. The prechase (time-zero) level of SL-Chk1$_{9m}$ in wild-type cells was ∼2.5-fold lower than in *ubr1Δ* cells (which lacked the Arg/N-end rule pathway), confirming that a large fraction of the endogenous SL-Chk1$_{9m}$ was destroyed by the Arg/N-end rule pathway in wild-type cells (*SI Appendix*, Fig. S3 *C* and *D*). Moreover, the prechase level of endogenous SL-Chk1$_{9m}$ was further decreased in *naa10Δ* cells, becoming ∼4.7-fold lower than in *ubr1Δ* cells (*SI Appendix*, Fig. S3 *C* and *D*). These findings were qualitatively similar to the results with (moderately) overexpressed SL-Chk1$_{3f}$ (Fig. 2 *C* and *E* and *SI Appendix*, Fig. S2 *A*, *C*, and *D*).

Degradation of Chk1 in *naa10Δ* Cells Does Not Involve an N-Degron. Might a small unacetylated Nt-residue (such as Ser) followed by a bulky hydrophobic residue (such as Leu) function, in the contexts of SL-Chk1$_{3f}$ and *naa10Δ* cells, as a previously unknown N-degron? To address this question, we constructed position-1, 2 mutants of SL-Chk1$_{3f}$. Both wild-type SL-Chk1$_{3f}$ and its mutants SD-Chk1$_{3f}$ and SF-Chk1$_{3f}$ were predicted substrates of the NatA Nt-acetylase. In contrast, the SK-Chk1$_{3f}$ and SR-Chk1$_{3f}$ mutants were unlikely to be Nt-acetylated in wild-type cells, because a position-2 basic residue impedes Nt-acetylation in yeast. The PS-Chk1$_{3f}$ and SP-Chk1$_{3f}$ mutants, which contained Pro at positions 1 and 2, respectively, were not Nt-acetylated in wild-type cells (45).

The results with **XZ**-Chk1$_{3f}$ proteins (**X** = S, P; **Z** = L, D, F, K, R, P), including wild-type SL-Chk1$_{3f}$, were essentially indistinguishable. All these proteins were degraded relatively slowly in

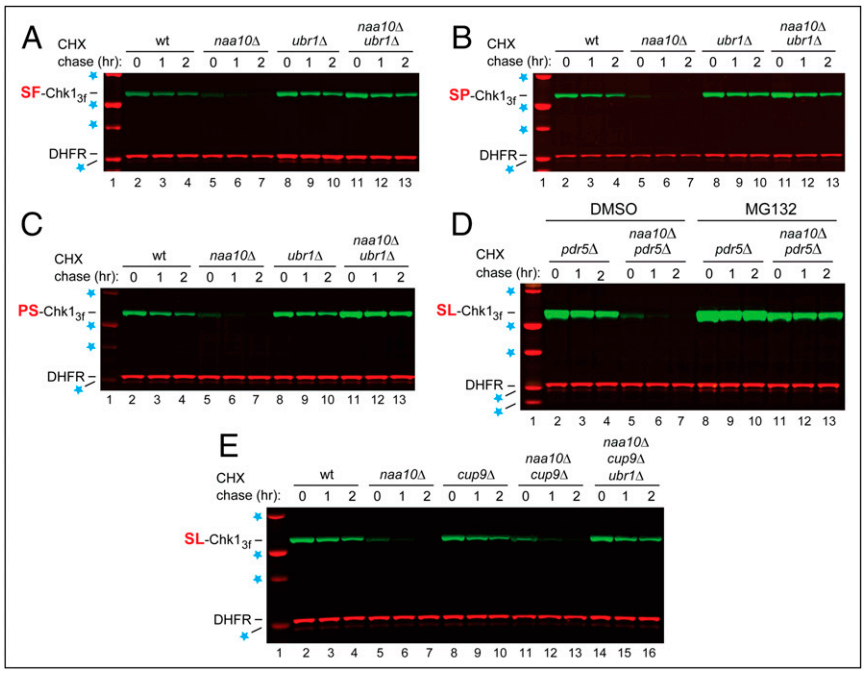

Fig. 4. Degradation of Chk1 mutants by the Arg/N-end rule pathway. (*A*) As in Fig. 2*D*, but with the SF-Chk1$_{3f}$ mutant. CHX-chases, using PRT (Fig. 2*B*), with SF-Chk1$_{3f}$, for 0, 1, and 2 h, with wild-type (lanes 2–4), *naa10Δ* (lanes 5–7), *ubr1Δ* (lanes 8–10), and *naa10Δ ubr1Δ* (lanes 11–13) *S. cerevisiae*. Blue stars are as in Fig. 2*D*. (*B*) As in *A* but with the SP-Chk1$_{3f}$ mutant. (*C*) As in *A* but with the PS-Chk1$_{3f}$ mutant. (*D*) Lanes 2–4, CHX-chase, using PRT (Fig. 2*B*), with wild-type SL-Chk1$_{3f}$, for 0, 1, and 2 h, in *pdr5Δ* cells. Lanes 5–7 are as in lanes 2–4 but in *pdr5Δ naa10Δ* cells. Lanes 8–10 and 11–13 are as in lanes 2–4 and 5–7, respectively, but in the presence of 50 μM MG132, a proteasome inhibitor. The absence of the Pdr5 multidrug transporter was necessary to make *S. cerevisiae* sensitive to MG132. Blue stars denote 20-, 25-, 37-, 50-, and 75-kDa markers. (*E*) CHX-chases, using PRT (Fig. 2*B*), with wild-type SL-Chk1$_{3f}$, for 0, 1, and 2 h, with wild-type (lanes 2–4), *naa10Δ* (lanes 5–7), *cup9Δ* (lanes 8–10), *naa10Δ cup9Δ* (lanes 11–13), and *naa10Δ cup9Δ ubr1Δ* (lanes 14–16) *S. cerevisiae*. Blue stars denote 25-, 37-, 50-, and 75-kDa markers.

wild-type cells, became much shorter-lived in *naa10Δ* cells, and required the Arg/N-end rule pathway for their degradation in *naa10Δ* cells (Figs. 2 *C–F* and 4 *A–C* and *SI Appendix*, Fig. S2 *E* and *F*). We concluded that **XZ**-Chk1$_{3f}$ (**X** = S, P; **Z** = L, D, F, K, R, P), including wild-type SL-Chk1$_{3f}$, were targeted by the Arg/N-end rule pathway in *naa10Δ* cells through an internal degron, which was largely inactive in wild-type cells (see below).

Hsp90 and Cochaperones as Substrates of the NatA Nt-Acetylase. Approximately 60% of proteins in the *S. cerevisiae* proteome are predicted substrates of NatA (Naa10) (*SI Appendix*, Fig. S1) (45). A parsimonious explanation of the accelerated degradation of SL-Chk1$_{3f}$ in *naa10Δ* (NatA-lacking) cells is that in wild-type cells SL-Chk1$_{3f}$ is shielded from the Arg/N-end rule pathway by a protective entity that becomes impaired in the absence of Nt-acetylation by NatA. Given the moderate overexpression of SL-Chk1$_{3f}$ in our assays (Fig. 2*B*), a protective entity had to be relatively abundant. The leading candidate was Hsp90, inasmuch as SL-Chk1 is a putative client of Hsp90 (55).

Hsc82 and Hsp82 are two similar *S. cerevisiae* Hsp90 chaperones (5, 8). Remarkably, our survey of the yeast Hsp90 system showed that not only Hsc82 and Hsp82, but also their cochaperones Aha1, Cdc37, Cns1, Cpr6, Cpr7, Hch1, Pih1, Ppt1, Rvb1, Rvb2, Sba1, Sse1, Sse2, Sti1, and Tah1 were either identified or predicted substrates of the NatA Nt-acetylase (*SI Appendix*, Figs. S1 and S5).

A bias this high was, a priori, an unlikely finding, because only ∼60% of the *S. cerevisiae* proteome are either identified or predicted substrates of NatA (45). It is unknown whether the observed near-exclusive preference for NatA by the Hsp90 system (*SI Appendix*, Figs. S1 and S5) is functionally adaptive, i.e., whether this bias was caused by natural selection. The alternative interpretation is that this pattern resulted largely from a "fluctuation" in a quasi-neutral genetic drift. In either case, these results (*SI Appendix*, Fig. S5) were consistent with the relevance of Hsp90 to degradation of SL-Chk1$_{3f}$ in *naa10Δ* cells (Fig. 2 *C* and *E* and *SI Appendix*, Fig. S2 *A*, *C*, and *D*).

Faster Degradation of Chk1 in Cells Containing Lower Levels of Hsp90. If destabilization of SL-Chk1$_{3f}$ in *naa10Δ* cells is caused by a lower Hsp90 activity, a decreased level of Hsp90 would be expected to accelerate the degradation of SL-Chk1$_{3f}$ in Naa10$^+$ cells. *S. cerevisiae* Hsp90 is encoded by the constitutive *HCS82* and the stress-inducible *HSP82*, whose single nulls (but not a double null) yield viable cells (8). Immunoblotting-based comparisons of the levels of Hsc82+Hsp82 in wild-type cells vs. *hsc82Δ*, *hsp82Δ*, and other mutants are shown in *SI Appendix*, Fig. S3 *D* and *E*. We also found that SL-Chk1$_{3f}$ was indeed destabilized in either *hsc82Δ* cells or *hsp82Δ* cells but not as strongly as in *naa10Δ* cells (*SI Appendix*, Fig. S3 *A* and *B*).

Ablation of Hsp90 Cochaperones Can Destabilize Chk1. We also found that SL-Chk1$_{3f}$ was shorter lived in Naa10$^+$ cells lacking the cochaperones Sba1, Sse1, Sti1, or Tah1 (*SI Appendix*, Fig. S6 *A* and *B*). These assays used Tc-PRT chases (Fig. 2 *A* and *B*). Tc is at most weakly toxic, in contrast to highly toxic cycloheximide (CHX). The basal degradation of SL-Chk1$_{3f}$ was faster in Tc-chases than in CHX-chases (e.g., compare Fig. 2 *C* and *E* with *SI Appendix*, Fig. S6*C*). The cause of this difference was traced to the in vivo degradation of the Ubr1 N-recognin (a study of this aspect of the Arg/N-end rule pathway is under way). Although chases that used CHX (at present the standard translation inhibitor for degradation assays in the Ub field) produced results qualitatively similar to those with Tc, all chases at later stages of the present study were done using Tc, for the reason above.

Hsp90 Itself and Other Proteins as Substrates of Ubr1 in *naa10Δ* Cells. We also examined other, quasi-randomly chosen non-Chk1 proteins for their degradation in *naa10Δ* cells vs. *ubr1Δ* cells. The Ubr1 targets thus identified were Kar4, a transcriptional regulator of pheromone responses; Tup1, a transcriptional corepressor; Gpd1, glycerol-3-phosphate dehydrogenase; Ste11, a kinase regulator of pheromone responses; and also, remarkably, Hsc82, the main Hsp90 chaperone (Fig. 3 *D* and *E* and *SI Appendix*, Figs. S3 *E* and *F*, S6*D*, and S7). Tup1 and Ste11 are clients of Hsp90 (56); Kar4 and Gpd1 may also be Hsp90 clients; and Hsc82 is itself an Hsp90.

The illuminating result that the Hsp90 (Hsc82) chaperone becomes vulnerable to the Arg/N-end rule pathway in *naa10Δ* cells (Fig. 3 *D* and *E*, and *SI Appendix*, Fig. S7 *C* and *D*) was in agreement with a technically independent finding, that the level of Hsc82+Hsp82 in *naa10Δ* cells was approximately twofold

lower than in wild-type cells (*SI Appendix*, Fig. S4 *D* and *E*). Together, these findings strongly suggested that newly formed Hsc82 and Hsp82 are themselves clients of mature Hsc82/Hsp82, requiring the (unimpaired) Hsp90 system for their conformational maturation and protection from the Arg/N-end rule pathway. The Ubr1-mediated degradation of Hsc82 (Fig. 3 *D* and *E* and *SI Appendix*, Figs. S4 *D* and *E* and S7 *C* and *D*) would account, at least in part, for the decreased protection, in *naa10Δ* cells, of Hsp90 clients such as SL-Chk1$_{3f}$ (Fig. 2 *C* and *E*).

As already observed with SL-Chk1$_{3f}$, one aspect of the Ubr1-dependent patterns of degradation of Kar4, Tup1, Gpd1, Ste11, and Hsc82 was a significant increase in the prechase (time-zero) level of a test protein in *ubr1Δ* cells (which lacked the Arg/N-end rule pathway), as compared with, e.g., *naa10Δ* cells. Particularly clear examples of this increase were Hsc82, Ste11, and Gpd1 (Fig. 3 *D* and *E* and *SI Appendix*, Figs. S6*D* and S7).

A parsimonious interpretation of the relative flatness of decay curves in some of these cases (e.g., *SI Appendix*, Fig. S6*D*), with the major change being a time-zero (prechase) alteration, is that "young" molecules of a protein (either cotranslationally or shortly after translation) are particularly vulnerable to the Arg/N-end rule pathway. The subsequent folding and quaternary structure formation (for example, mature Gpd1 is a homodimer) would make these proteins either partly or completely resistant to the Ubr1-mediated degradation through the shielding of a cognate degron and/or through a higher resistance to the unfolding of a targeted protein by the 26S proteasome. Conformational maturation of the above (and other) proteins can be partly reversible and takes place, at least in part, through their (protective) interactions with the Hsp90 system. Thus impairment of Hsp90 in *naa10Δ* cells increases the vulnerability of some Hsp90 clients, such as conditional Ubr1 substrates, to attacks by the Arg/N-end rule pathway.

An extensively analyzed precedent for the non–first-order (nonexponential) degradation kinetics by the Arg/N-end rule pathway was X–β-galactosidase (X–β-gal) bearing a destabilizing N-terminal residue (18). These first (engineered) Arg/N-end rule substrates were vulnerable to the targeting by Ubr1 cotranslationally and/or shortly after translation. The subsequent formation of an X–β-gal homotetramer led to the nearly (but not quite) complete cessation of the degradation of a "mature" X–β-gal tetramer by the Arg/N-end rule pathway (15, 18, 19). Later studies have shown that a non–first-order degradation kinetics is also a frequent aspect of proteolysis by the Ub system at large, resulting, primarily, from the same causes of time-dependent protein folding and formation of protein complexes (44, 57–59).

As shown below, Ubr1 recognizes an internal, C terminus-proximal degron of SL-Chk1. It is likely (but remains to be verified) that Kar4, Tup1, Gpd1, Ste11, and Hsc82 also bear Ubr1-specific internal degrons (as distinguished from N-degrons). Overall, ∼60% of 11 examined yeast proteins were identified as substrates of the Arg/N-end rule pathway in *naa10Δ* cells. Given this percentage and the quasi-random selection of proteins for these experiments, it is possible, indeed likely, that roughly a half of natural Hsp90 clients, i.e., ∼10% of the cellular proteome, will eventually be identified as conditional (Hsp90 state-dependent) substrates of the Arg/N-end rule pathway.

Overexpression of Ubr1–Ufd4 Destabilizes Chk1 in Wild-Type Cells. Natural levels of Ubr1 are rate-limiting in the Arg/N-end rule pathway (15). We therefore asked whether co-overexpression of Ubr1 and Ufd4, two interacting Ub ligases of the Arg/N-end rule pathway (Fig. 1*B*), might accelerate the degradation of SL-Chk1$_{3f}$ in wild-type cells, despite the presence of the NatA Nt-acetylase. Remarkably, we found that they did so (Fig. 5 *A* and *B*). This result strongly suggested that the rate of degradation of an Hsp90 client such as SL-Chk1$_{3f}$ is determined by a dynamic partitioning of SL-Chk1$_{3f}$ between a protected Hsp90-bound state and a "free" state vulnerable to the Arg/N-end rule pathway.

The Endogenous Arg/N-End Rule Pathway Is Up-Regulated in *naa10Δ* Cells. We also asked whether the Arg/N-end rule pathway might become naturally up-regulated in *naa10Δ* cells, which exhibited the accelerated degradation of SL-Chk1$_{3f}$ (Fig. 2 *C* and *E* and *SI Appendix*, Fig. S3 *A*, *C*, and *D*). We began by comparing, using an affinity-purified antibody to *S. cerevisiae* Ubr1 (60), the levels of Ubr1 in wild-type vs. *naa10Δ* cells, with *ubr1Δ* cells as a negative control (Fig. 3 *B* and *C*). Despite the high sensitivity of this antibody [it could detect, by immunoblotting, down to ∼2 ng of Ubr1 (60)], the levels of endogenous Ubr1 in wild-type cells [500–1,000 Ubr1 molecules per haploid cell in exponential growth (38)] were low enough to make these measurements technically challenging. Nevertheless, we reproducibly observed an ∼2.5-fold increase of the endogenous, untagged Ubr1 in *naa10Δ* cells as compared with wild-type cells (Fig. 3 *B* and *C*).

In a conceptually independent set of assays, we used X–β-gal (in which **X** = His or Tyr) as Ub fusion-based reporters of the Arg/N-end rule pathway (15, 18, 19). N-terminal His and Tyr are recognized by Ubr1 through its type-1 site (this site binds to basic Nt-residues) and type-2 site (this site binds to bulky hydrophobic Nt-residues), respectively (Fig. 1*B*). In agreement with the higher levels of Ubr1 in *naa10Δ* cells (Fig. 3 *B* and *C*), the degradation of His–β-gal and Tyr–β-gal was much faster in *naa10Δ* cells than in wild-type cells (see Fig. 7 *C*–*E*). A strong up-regulation of the Arg/N-end rule pathway in the absence of NatA provides a glimpse of still unexplored circuits that regulate the levels of pathway's components and the activity of this proteolytic system.

Mapping the Chk1 Degron by Degradation Assays. Having determined that the targeting of SL-Chk1$_{3f}$ did not involve an N-degron (Figs. 2 *C*–*F* and 4 *A*–*C*, and *SI Appendix*, Fig. S2 *E* and *F*), we mapped an internal degron of Chk1 by examining its C-terminally truncated derivatives (*SI Appendix*, Fig. S8). Except for SL-Chk1$^{1–502}_{3f}$ and SL-Chk1$^{1–465}_{3f}$, the truncated derivatives of SL-Chk1$^{1–527}_{3f}$ could not be expressed in reference-based PRT assays at readily detectable levels in either wild-type or *ubr1Δ* cells (*SI Appendix*, Fig. S8), suggesting their rapid (and Ubr1-independent) destruction, likely as the result of their misfolding. The absence, in SL-Chk1$^{1–502}_{3f}$, of only 25 C-terminal residues of wild-type SL-Chk1$^{1–527}_{3f}$ abolished a decreased prechase level of Chk1 in *naa10Δ* cells and also nearly sufficed to eliminate the dependence of degradation on Ubr1 (*SI Appendix*, Fig. S6 *A* and *B*). SL-Chk1$^{1–465}_{3f}$ yielded similar results, except that the effect of Ubr1 was now completely gone (*SI Appendix*, Fig. S6 *A* and *C*). Thus, a degron recognized by Ubr1 is located largely within the last 25 residues of the 527-residue Chk1.

Mapping the Chk1 Degron by Two-Hybrid Binding Assays. We recently used two-hybrid assays (61) to map the recognition of a degron by its cognate E3 Ub ligase (21). Application of this method to interactions between Chk1 and the Ubr1 E3 is shown in Fig. 6*A*. Controls included immunoblotting to verify the expression of two-hybrid fusions and also confirming that binding-positive fusions did not stay positive in assays with one of two fusions (e.g., *SI Appendix*, Fig. 6 *A*, *1*). In agreement with truncation-degradation assays (*SI Appendix*, Fig. S6), the in vivo interaction between Ubr1 and the 527-residue Chk1 could be abrogated by deleting the last 25 residues of Chk1 (Fig. 6*A*).

Mapping the Chk1 Degron by Split-Ubiquitin Binding Assays. In addition and independently, Ubr1–Chk1 interactions were also analyzed by the split-Ub assay. In this method, test proteins are expressed as fusions, respectively, to a C-terminal half of Ub (C_{ub}) and to its mutant N-terminal half (N_{ub}). Interactions between test proteins would reconstitute a quasi-native Ub moiety from C_{ub} and mutant N_{ub}. The resulting cleavage of a C_{ub}-containing fusion by deubiquitylases downstream from the Ub moiety serves as a readout of this technique (62, 63).

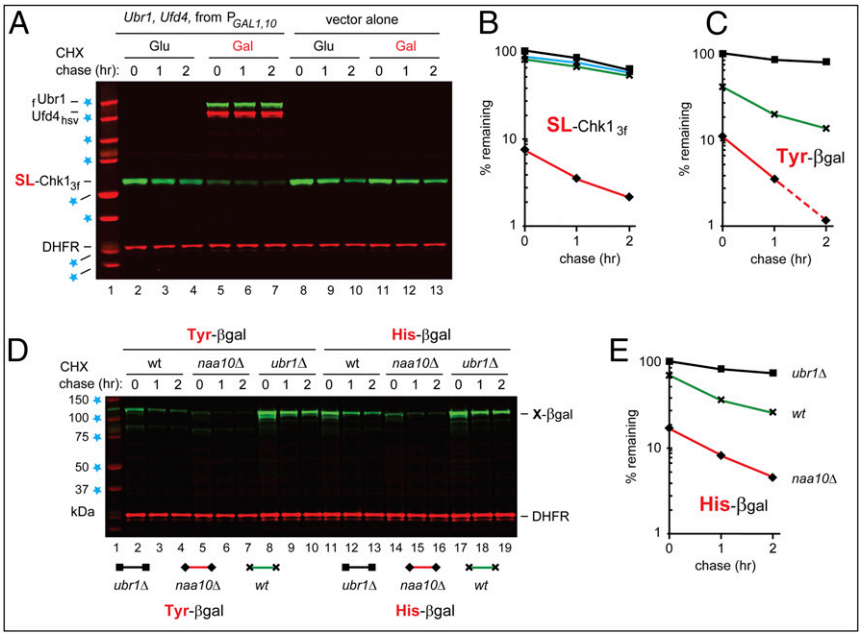

Fig. 5. Overexpression of the Arg/N-end rule pathway destabilizes Chk1. (*A*) CHX-chases, using PRT (Fig. 2*B*), with wild-type SL-Chk1$_{3f}$, for 0, 1, and 2 h, in wild-type *S. cerevisiae* carrying a high-copy plasmid that expressed both flag-tagged Ubr1 ($_f$Ubr1) and Hsv-tagged Ufd4 (Ufd4$_{hsv}$) from the bidirectional P$_{GAL1,10}$ promoter. Lanes 2–4 and 5–7: cells containing the P$_{GAL1,10}$-*UBR1/UFD4* plasmid in glucose and galactose medium, respectively. Lanes 8–10 and 11–13 are as in lanes 2–4 and 5–7, respectively, but with cells containing a vector alone. The presence of $_f$Ubr1 and Ufd4$_{hsv}$ in lanes 5–7 was verified directly, using anti-flag and anti-Hsv antibodies. Blue stars denote 20-, 25-, 37-, 50-, 75-, 100-, 150-, and 250-kDa markers. (*B*) Quantification of data in *A*. Rhombuses, squares, triangles, and crosses denote, respectively, the decay curves of SL-Chk1$_{3f}$ in wild-type cells overexpressing Ubr1-Ufd4 (in galactose), or containing vector alone (in glucose), or containing the repressed Ubr1-Ufd4 plasmid (in glucose), or containing vector alone (in galactose). (*C*) Quantification of data in *D*, lanes 2–10. For curve designations, see the keys below the immunoblot in *D*. (*D*) Lane 1, kDa markers. CHX-chase, using PRT (Fig. 2*B*), for 0, 1, and 2 h, with wild-type (lanes 2–4), *naa10Δ* (lanes 5–7), and *ubr1Δ* (lanes 8–10) *S. cerevisiae* expressing Tyr–β-gal, derived from Ub–Tyr–β-gal. Lanes 11–19 are as in lanes 2–10 but with His–β-gal, derived from Ub–His–β-gal. Blue stars indicate 37-, 50-, 75-, 100-, and 150-kDa markers. (*E*) Quantification of data in *D*, lanes 11–19. For curve designations, see the keys below the immunoblot in *D*. All chases in this study were performed at least twice, yielding results that differed by less than 10%.

In agreement with truncation-degradation and two-hybrid assays (Fig. 6*A* and *SI Appendix*, Fig. S6), Ubr1 could bind, in split-Ub assays, to the full-length SL-Chk1$^{1–527}$ but not to SL-Chk1$^{1–502}$ (*SI Appendix*, Figs. S4*A* and 6 *B*, *1* and *4*). Moreover, the Ubr1-recognized region of SL-Chk1$^{1–527}$ may be as small as 10 or fewer C-terminal residues. Specifically, neither SL-Chk1$^{1–510}$ nor SL-Chk1$^{1–517}$ could bind to Ubr1, in contrast to wild-type SL-Chk1$^{1–527}$ (Fig. 6*B*).

Degron-Specific Ubiquitylation of Chk1 in a Defined in Vitro System. We also developed a ubiquitylation system that comprised the following purified *S. cerevisiae* proteins: His$_6$-Ub; the Uba1 E1 enzyme; the Rad6 E2 enzyme; the His$_6$–Ubc4 E2 enzyme; the C-terminally flag-tagged Ufd4$_f$ E3; the N-terminally flag-tagged $_f$Ubr1 E3; the C-terminally myc–flag-tagged full-length SL-Chk1$^{1–527}_{m–f}$; and also, alternatively, SL-Chk1$^{1–502}_{m–f}$, lacking the last 25 residues of Chk1 (Fig. 7*A*). This completely defined in vitro system could reproduce the recognition of Chk1 by Ubr1 that was inferred from truncation-degradation, two-hybrid, and split-Ub assays (Fig. 6 *A* and *B* and *SI Appendix*, Fig. S6). SL-Chk1$^{1–527}_{m–f}$ was polyubiquitylated if the system contained ATP, Ub, Uba1, and at least Ubr1 and Rad6. Ufd4 and Ubc4 had no effect in this system, and Ufd4–Ubc4 by themselves, in the absence of Ubr1, did not support polyubiquitylation of SL-Chk1$^{1–527}_{m–f}$ (Fig. 7 *B* and *C*). Crucially, the complete system containing SL-Chk1$^{1–502}_{m–f}$, which lacked the 25 C-terminal residues of SL-Chk1$^{1–527}_{m–f}$, could polyubiquitylate the latter but not the former protein (Fig. 7*C*, lane 12).

In agreement with degron-mapping results (Figs. 6 *A* and *B* and 7 and *SI Appendix*, Fig. S6), alignments of Chk1 amino acid sequences from several yeasts (*S. cerevisiae*, *Candida glabrata*, *Lachancea fermentati*, and *Kluyveromyces lactis*) revealed a particularly strong conservation of the last ∼25 residues, in comparison, e.g., with the next ∼30 residues upstream of that region (Fig. 6*D*). The few divergences over the last 25 residues of Chk1 involved solely changes to similar residues (Fig. 6*D*). In sum, the minimal degron of SL-Chk1$^{1–527}$ comprises its ∼10 C-terminal residues (Fig. 5*B*), but the complete degron is larger, as suggested, in particular, by a weak but detectable Ubr1 dependence of the degradation of SL-Chk1$^{1–502}$, which lacked the last 25 residues of Chk1 (*SI Appendix*, Fig. S8*B*).

Chk1-Hsp90 Interactions in Wild-Type but Not in *naa10Δ* Cells. We found that split-Ub assays (62, 63) could also detect in vivo interactions between full-length Chk1 and Hsc82, the main Hsp90 chaperone (Fig. 6 *C*, *1* and *2* and *SI Appendix*, Fig. S4 *B*, *3*). This detection required the absence of obstruction of the C terminus of the Hsc82 moiety. Specifically, a split-Ub configuration in which the C terminus of Hsc82 was linked to the C$_{ub}$-activator moiety yielded a barely detectable signal (*SI Appendix*, Fig. S4 *B*, *3* and *4*), in agreement with the importance of the C terminus of Hsc82, including its dimerization and its interactions with cochaperones (8).

Remarkably, the same split-Ub assays that yielded a robust Chk1–Hsc82 interaction signal in wild-type cells produced virtually no interaction signal in *naa10Δ* cells (Fig. 6*C* and *SI Appendix*, Fig. S4*C*). This striking difference could not be caused by a failure of the split-Ub assay itself, because the interactions between Ubr1 and Chk1 were readily detected by split-Ub in either wild-type or *naa10Δ* cells (*SI Appendix*, Fig. S4 *B*, *1* and *2*).

The near-abrogation of the in vivo binding of Chk1 to its protector Hsc82 in *naa10Δ* cells (in contrast to wild-type cells) illuminated still another aspect of the impairment of the Hsp90 system

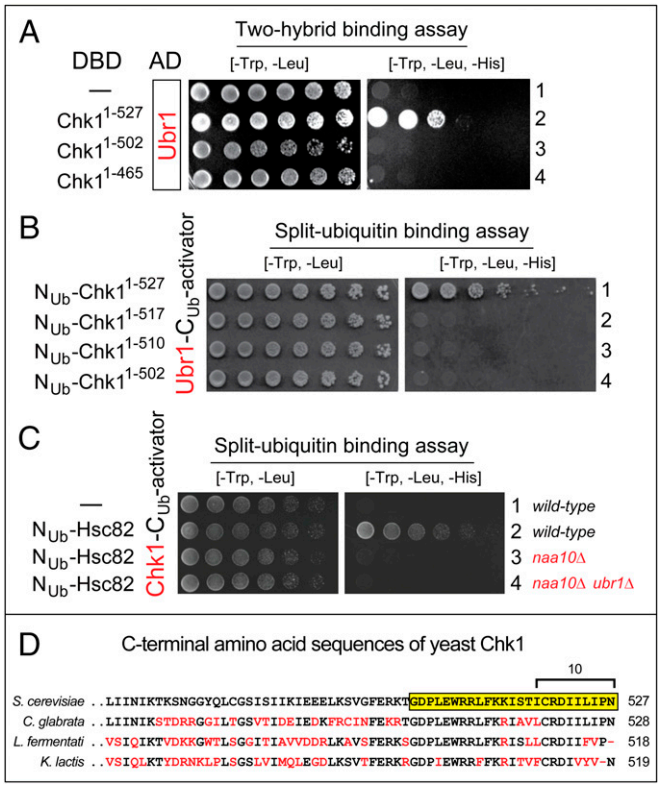

Fig. 6. Mapping Chk1 degron by two-hybrid and split-ubiquitin assays. (*A*) Two-hybrid binding assays with Ubr1 vs. Chk1. In both two-hybrid and split-Ub assays, the expression of *HIS3* (the ultimate readout of both assays), in otherwise His^- cells, was a function of affinity between test proteins. (*A–C*, *Left*) Images of His-containing plates, on which all yeast strains grew. (*Right*) His-lacking plates, on which only His^+ cells grew. A two-hybrid-based Ubr1 fusion bearing the activation domain (AD) was examined vs. full-length $Chk1^{1–527}$ and its truncated derivatives bearing the DNA-binding domain (DBD). (*A*, *1*) Ubr1 alone (negative control). (*A*, *2*) Full-length $Chk1^{1–527}$ vs. Ubr1. (*A*, *3*) $Chk1^{1–502}$ vs. Ubr1. (*A*, *4*) $Chk1^{1–465}$ vs. Ubr1. (*B*) Split-Ub binding assays with Ubr1 vs. Chk1. Split-Ub–based fusions (*Materials and Methods*) of Ubr1 vs. $Chk1^{1–527}$, $Chk1^{1–517}$, $Chk1^{1–510}$, and $Chk1^{1–502}$. (*C*) Split-Ub binding assays with full-length Chk1 vs. full-length Hsc82 in wild-type, *naa10Δ*, and *naa10Δ ubr1Δ* cells. C1, Chk1 alone (negative control). (*D*) Alignment of C-terminal regions of Chk1 from the indicated yeast species. The last 25 residues of *S. cerevisiae* Chk1 are highlighted in yellow. The last 10 residues of Chk1 (found to be essential for the binding to Ubr1; see *C*, *2*) are marked as well. Residues of Chk1 in species other than *S. cerevisiae* that differed from those of *S. cerevisiae* Chk1 are in red.

in the absence of NatA. The mechanism of this effect (Fig. 6*C* and *SI Appendix*, Fig. S4*C*) remains to be understood. It may involve not only Hsc82 and Hsp82, because both they and their ∼15 cochaperones are either identified or predicted substrates of the NatA Nt-acetylase that is absent in *naa10Δ* cells.

Discussion

This study revealed a major impairment of the Hsp90 chaperone in *naa10Δ S. cerevisiae*, pinpointed causes of this perturbation, showed that the Arg/N-end rule pathway is strongly up-regulated in the absence of the NatA (Naa10) Nt-acetylase, identified several substrates of the Arg/N-end rule pathway, and suggested specific functions of Nt-acetylation in the physiological regulation of the Hsp90 system. In the absence of the NatA Nt-acetylase, roughly 2,000 normally Nt-acetylated yeast proteins lack this modification (45). In particular, the entire Hsp90 system (Hsc82, Hsp82, and its ∼15 cochaperones) would not be Nt-acetylated in *naa10Δ* cells (*SI Appendix*, Fig. S5).

One manifestation of Hsp90 impairment in *naa10Δ* cells was a much faster degradation of Chk1 (a mitotic checkpoint kinase and Hsp90 client) by the Arg/N-end rule pathway, which was found to recognize a specific C terminus-proximal degron of Chk1 (Figs. 1*B*, 2, 6, and 7). The protection of Chk1 by Hsp90 could be overridden not only by the absence of the NatA Nt-acetylase but also by overexpression of the Arg/N-end rule pathway in wild-type cells (Fig. 5 *A* and *B*). This result indicated that the rate of degradation of Chk1 is determined by its dynamic partitioning between a protected Hsp90-bound state and a free state vulnerable to the Arg/N-end rule pathway. Therefore it was possible that the Arg/N-end rule pathway might be naturally up-regulated in *naa10Δ* cells, because that upregulation would account, at least in part, for the observed destabilization of Chk1 in these cells. The Arg/N-end rule pathway was indeed found to be much more active in *naa10Δ* cells than in wild-type cells (Figs. 3 *B* and *C* and 5 *C–E*).

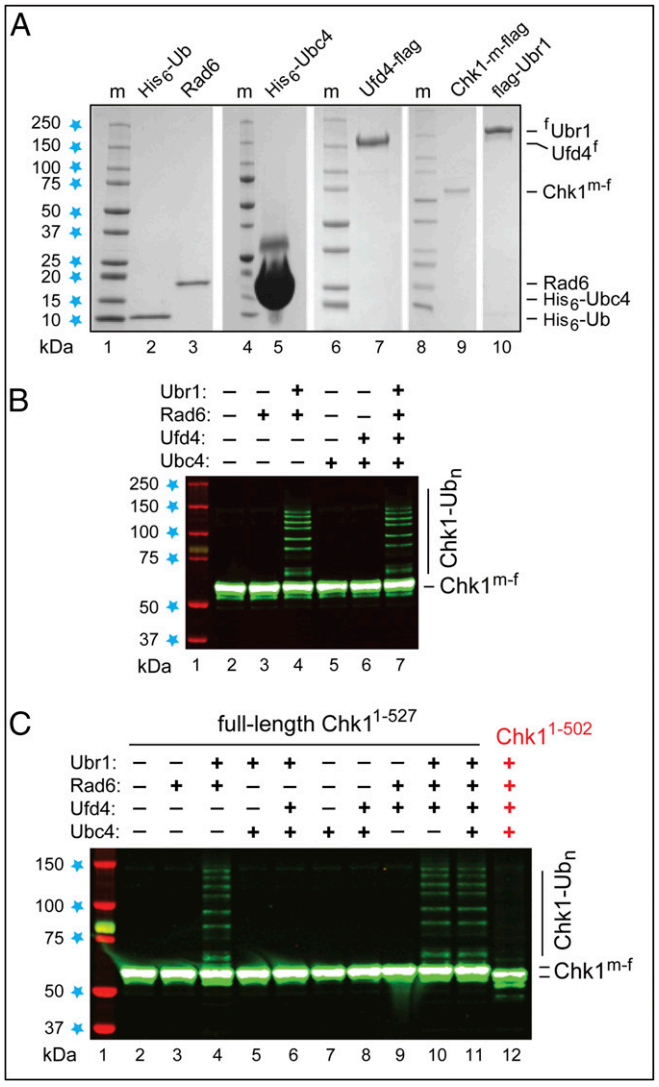

Fig. 7. Degron-specific polyubiquitylation of Chk1 in a defined in vitro system. (*A*) Coomassie-stained SDS/PAGE patterns of purified *S. cerevisiae* His_6-Ub, Rad6, His_6-Ubc4, $Ufd4_f$, full-length $SL\text{-}Chk1^{1–527}_{m–f}$, and $_f$Ubr1. (*B*) Lane 1, kDa markers. Lanes 2–7, $SL\text{-}Chk1^{1–527}_{m–f}$ incubated in the presence of ATP, Ub, Uba1, and other purified proteins as indicated. Immunoblotting with anti-flag antibody. (*C*) As in *B* but independent Chk1 polyubiquitylation assays that included, in addition, the assay with C-terminally truncated $SL\text{-}Chk1^{1–502}_{m–f}$ (lane 12).

Yet another result that revealed a distinct cause of Hsp90 impairment in the absence of NatA was the degradation of Hsc82, the main Hsp90 chaperone, by the Arg/N-end rule pathway in *naa10Δ* cells and the corresponding (approximately twofold) decrease in the steady-state level of Hsc82+Hsp82 in the absence NatA, relative to wild-type cells (Fig. 3 *D* and *E* and *SI Appendix*, Fig. S7 *C* and *D*). The degradation of the Hsp90 chaperone (Hsc82 and presumably Hsp82 as well) by the Arg/N-end rule pathway in *naa10Δ* cells accounts, at least in part and independently of other causes, for the decreased protection of Hsp90 clients under these conditions.

These and related results strongly suggested three causes of the Hsp90 impairment in *naa10Δ* cells that are not mutually exclusive. A fourth cause, also stated below, is hypothetical but verifiable and would be physiologically important if correct.

i) A strongly increased activity of the Arg/N-end rule pathway in the absence of NatA and, consequently, an increased ability of this pathway to compete with Hsp90 for its clients such as, for example, Chk1. This finding (Figs. 3 *B* and *C*, and 5 *C*–*E*) provides a glimpse of still unexplored circuits that regulate components of the Arg/N-end rule pathway and its proteolytic activity.

ii) An intrinsic weakening of Hsp90 in *naa10Δ* cells, because nearly all its components (Hsc82, Hsp82, and their ∼15 cochaperones) are NatA substrates (*SI Appendix*, Fig. S5). The resulting impairment of protein interactions that normally involve the Nt-Ac groups of Nt-acetylated proteins (see the Introduction) is likely to underlie the observed degradation of Hsp90 (Hsc82) by the Arg/N-end rule pathway in *naa10Δ* cells (Fig. 3 *D* and *E* and *SI Appendix*, Figs. S4 *D* and *E* and S5 *C* and *D*).

iii) In addition to a decreased steady-state level of the Hsc82 (Hsp90) protein in *naa10Δ* cells (see item *ii* above), one would also expect the impairment of the Hsp90 system as a whole in the absence of NatA. The functioning of Hsp90 involves its transient binding to cochaperones, with some of them carrying bound clients (12). Given the role of Nt-Ac groups in modulating (usually enhancing) protein interactions within cognate protein complexes (49), decreased affinities among most components of the Hsp90 system, which are not Nt-acetylated in *naa10Δ* cells, would be expected to perturb both the delivery of clients to Hsp90 by cochaperones and other aspects of this circuit, based on transient protein interactions.

Our detection, via split-Ub assays in wild-type cells, of the in vivo interaction between Hsp90 (Hsc82) and its client Chk1 and the remarkable near-ablation of this interaction in *naa10Δ* cells (Fig. 6*C* and *SI Appendix*, Fig. S4*B*, *3* and *4*) strongly support this view of the Hsp90 system in cells lacking NatA.

iv) The absence of a normally present Nt-Ac group in a subunit of a protein complex can decrease the subunit's affinity for the rest of the complex from ∼10-fold to ∼1,000-fold (48, 49). Thus, the numerous and normally Nt-acetylated *S. cerevisiae* proteins that lack this modification in *naa10Δ* cells would form otherwise cognate in vivo complexes that would be prone to (reversible) dissociation. Away from their natural protein ligands, at least some dissociated free subunits would be likely to act as conformationally disordered Hsp90 clients, thereby competing with normal Hsp90 clients and, consequently, impairing protein homeostasis for that reason alone. Note that some of these free proteins, dissociated from complexes that would be less stable in *naa10Δ* cells, may even not require assistance by Hsp90 cochaperones for binding to Hsp90. (The fraction of in vivo Hsp90 clients that can interact with Hsp90 directly, without their initial binding to cochaperones, is not known.) This fourth mechanism of Hsp90 impairment in *naa10Δ* cells remains to be addressed experimentally.

One feature of *naa10Δ S. cerevisiae* is the remarkably broad range of this mutant's abnormal phenotypes. They include cell-cycle and mating defects as well as temperature sensitivity and perturbations of protein synthesis and degradation (27, 46, 64). Our finding of specific connections between the Hsp90-mediated protein homeostasis and the Nt-acetylation of proteins by NatA has revealed a major reason for the multiplicity of *naa10Δ* effects, given the wide range of Hsp90 functions and their impairment in the absence of NatA. Strong evolutionary conservation of the Hsp90 system, Nt-acetylases, and N-end rule pathways indicates that the results of this study are also relevant to multicellular eukaryotes, including mammals.

Given the advances described above, an important question is whether a perturbation of the Hsp90 system that is similar to the impairment observed with *naa10Δ S. cerevisiae* can also occur in nonmutational settings. Decreased NatA activity can be caused, for example, by a stress-mediated down-regulation of Ac-CoA, the co-substrate of Nt-acetylases. Indeed, physiologically relevant changes in the levels of Ac-CoA have been shown to affect both the efficacy of Nt-acetylation and the sensitivity of mammalian cells to apoptotic signals (65). It would be illuminating, therefore, to determine a role that the Hsp90 system plays in specific connections between Ac-CoA, Nt-acetylation, and apoptosis, particularly because the Arg/N-end rule pathway has already been shown to be a regulator of apoptosis (22, 29).

Changes in the rate of Nt-acetylation of cellular proteins by NatA can also be caused by altered levels of the NatA Nt-acetylase and/or changes in its enzymatic activity. The expression of NatA in the plant *Arabidopsis thaliana* and, correspondingly, the in vivo Nt-acetylation of NatA substrates have been found to be controlled by the phytohormone abscisic acid (66). Remarkably, a natural decrease of NatA during drought was shown to be required for plants' tolerance to drought (66). Analogous regulated changes in the levels of NatA and/or Ac-CoA, as well as connections between these changes and either the Hsp90 system or the Arg/N-end rule pathway, remain to be explored in other organisms, including mammals.

Materials and Methods

For further information, see *SI Appendix, SI Materials and Methods*.

Yeast Strains, Media, and Genetic Techniques. The *S. cerevisiae* strains used in this work are described in *SI Appendix*, Table S1. Standard techniques were used for strain construction and transformation. *S. cerevisiae* media included yeast extract/peptone/dextrose (YPD) and Synthetic Complete (SC) medium (Sigma-Aldrich).

Construction of Plasmids. The plasmids used in this study are described in *SI Appendix*, Table S2. Construction details are described in *SI Appendix, SI Materials and Methods*. All final constructs were verified by DNA sequencing.

PRT-Based CHX-Chases, Tc-Chases, and ^{35}S-Pulse-Chase Assays. The PRT method is described in Fig. 2 *A* and *B*. Details of PRT-based CHX-chases and Tc-chases are described in *SI Appendix, SI Materials and Methods*. Protein bands visualized by immunoblotting were quantified using an Odyssey-9120 Imaging System (LI-COR).

Two-Hybrid Assays. Yeast-based two-hybrid binding assays (61) were carried out largely as described previously (21). "AD" and "DBD" refer to activation domain and DNA-binding domain, respectively. In both two-hybrid and split-Ub assays (described below), the expression of *HIS3* (the ultimate readout of both assays), in otherwise His$^-$ cells, was a function of affinity between test proteins.

Split-Ub Assays. Yeast-based split-Ub binding assays (62, 63) were carried out largely as described previously (21).

In Vitro Ubiquitylation Assay. Protein components of the assay were expressed in *Escherichia coli* or *S. cerevisiae*. The assay was carried as described in *SI Appendix, SI Materials and Methods*.

ACKNOWLEDGMENTS. We thank A. Melnykov, I. Printsev, and T. T. M. Vu (California Institute of Technology) for their comments on the manuscript and the present and former members of the A.V. laboratory for their assistance and advice. This work was supported by NIH Grants GM031530 and DK039520 (to A.V.).

1. Hartl FU, Bracher A, Hayer-Hartl M (2011) Molecular chaperones in protein folding and homeostasis. *Nature* 475:324–332.
2. Horwich AL (2014) Molecular chaperones in cellular protein folding: The birth of a field. *Cell* 157:285–288.
3. Wolff S, Weissman JS, Dillin A (2014) Differential scales of protein quality control. *Cell* 157:52–64.
4. Powers ET, Balch WE (2013) Diversity in the origins of proteostasis networks—a driver for protein function in evolution. *Nat Rev Mol Cell Biol* 14:237–248.
5. Borkovich KA, Farrelly FW, Finkelstein DB, Taulien J, Lindquist S (1989) hsp82 is an essential protein that is required in higher concentrations for growth of cells at higher temperatures. *Mol Cell Biol* 9:3919–3930.
6. Karagöz GE, Rüdiger SGD (2015) Hsp90 interaction with clients. *Trends Biochem Sci* 40:117–125.
7. Li J, Buchner J (2013) Structure, function and regulation of the hsp90 machinery. *Biomed J* 36:106–117.
8. Leach MD, Klipp E, Cowen LE, Brown AJ (2012) Fungal Hsp90: A biological transistor that tunes cellular outputs to thermal inputs. *Nat Rev Microbiol* 10:693–704.
9. Echeverría PC, Bernthaler A, Dupuis P, Mayer B, Picard D (2011) An interaction network predicted from public data as a discovery tool: Application to the Hsp90 molecular chaperone machine. *PLoS One* 6:e26044.
10. Prodromou C (2012) The 'active life' of Hsp90 complexes. *Biochim Biophys Acta* 1823: 614–623.
11. Mayer MP, Le Breton L (2015) Hsp90: Breaking the symmetry. *Mol Cell* 58:8–20.
12. Verba KA, et al. (2016) Atomic structure of Hsp90-Cdc37-Cdk4 reveals that Hsp90 traps and stabilizes an unfolded kinase. *Science* 352:1542–1547.
13. Geiler-Samerotte KA, Zhu YO, Goulet BE, Hall DW, Siegal ML (2016) Selection transforms the landscape of genetic variation interacting with Hsp90. *PLoS Biol* 14: e2000465.
14. Taipale M, Jarosz DF, Lindquist S (2010) HSP90 at the hub of protein homeostasis: Emerging mechanistic insights. *Nat Rev Mol Cell Biol* 11:515–528.
15. Varshavsky A (2011) The N-end rule pathway and regulation by proteolysis. *Protein Sci* 20:1298–1345.
16. Tasaki T, Sriram SM, Park KS, Kwon YT (2012) The N-end rule pathway. *Annu Rev Biochem* 81:261–289.
17. Gibbs DJ, Bacardit J, Bachmair A, Holdsworth MJ (2014) The eukaryotic N-end rule pathway: Conserved mechanisms and diverse functions. *Trends Cell Biol* 24: 603–611.
18. Bachmair A, Finley D, Varshavsky A (1986) In vivo *h*alf-life of a protein is a function of its amino-terminal residue. *Science* 234:179–186.
19. Bachmair A, Varshavsky A (1989) The degradation signal in a short-lived protein. *Cell* 56:1019–1032.
20. Hwang CS, Shemorry A, Varshavsky A (2010) N-terminal acetylation of cellular proteins creates specific degradation signals. *Science* 327:973–977.
21. Chen SJ, Wu X, Wadas B, Oh J-H, Varshavsky A (2017) An N-end rule pathway that recognizes proline and destroys gluconeogenic enzymes. *Science* 355:366.
22. Eldeeb M, Fahlman R (2016) The-N-end rule: The beginning determines the end. *Protein Pept Lett* 23:343–348.
23. Dougan DA, Micevski D, Truscott KN (2012) The N-end rule pathway: From recognition by N-recognins, to destruction by AAA+proteases. *Biochim Biophys Acta* 1823: 83–91.
24. Mogk A, Schmidt R, Bukau B (2007) The N-end rule pathway for regulated proteolysis: Prokaryotic and eukaryotic strategies. *Trends Cell Biol* 17:165–172.
25. Piatkov KI, Vu TTMH, Hwang CS, Varshavsky A (2015) Formyl-methionine as a degradation signal at the N-termini of bacterial proteins. *Microb Cell* 2:376–393.
26. Cha-Molstad H, et al. (2015) Amino-terminal arginylation targets endoplasmic reticulum chaperone BiP for autophagy through p62 binding. *Nat Cell Biol* 17:917–929.
27. Kim HK, et al. (2014) The N-terminal methionine of cellular proteins as a degradation signal. *Cell* 156:158–169.
28. Park SE, et al. (2015) Control of mammalian G protein signaling by N-terminal acetylation and the N-end rule pathway. *Science* 347:1249–1252.
29. Piatkov KI, Brower CS, Varshavsky A (2012) The N-end rule pathway counteracts cell death by destroying proapoptotic protein fragments. *Proc Natl Acad Sci USA* 109: E1839–E1847.
30. Brower CS, Piatkov KI, Varshavsky A (2013) Neurodegeneration-associated protein fragments as short-lived substrates of the N-end rule pathway. *Mol Cell* 50:161–171.
31. Yamano K, Youle RJ (2013) PINK1 is degraded through the N-end rule pathway. *Autophagy* 9:1758–1769.
32. Choi WS, et al. (2010) Structural basis for the recognition of N-end rule substrates by the UBR box of ubiquitin ligases. *Nat Struct Mol Biol* 17:1175–1181.
33. Kim MK, Oh SJ, Lee BG, Song HK (2016) Structural basis for dual specificity of yeast N-terminal amidase in the N-end rule pathway. *Proc Natl Acad Sci USA* 113: 12438–12443.
34. Wadas B, Piatkov KI, Brower CS, Varshavsky A (2016) Analyzing N-terminal arginylation through the use of peptide arrays and degradation assays. *J Biol Chem* 291: 20976–20992.
35. Hu R-G, et al. (2005) The N-end rule pathway as a nitric oxide sensor controlling the levels of multiple regulators. *Nature* 437:981–986.
36. Brower CS, Varshavsky A (2009) Ablation of arginylation in the mouse N-end rule pathway: Loss of fat, higher metabolic rate, damaged spermatogenesis, and neurological perturbations. *PLoS One* 4:e7757.
37. Kwon YT, et al. (2002) An essential role of N-terminal arginylation in cardiovascular development. *Science* 297:96–99.
38. Hwang CS, Shemorry A, Auerbach D, Varshavsky A (2010) The N-end rule pathway is mediated by a complex of the RING-type Ubr1 and HECT-type Ufd4 ubiquitin ligases. *Nat Cell Biol* 12:1177–1185.
39. Turner GC, Du F, Varshavsky A (2000) Peptides accelerate their uptake by activating a ubiquitin-dependent proteolytic pathway. *Nature* 405:579–583.
40. Eisele F, Wolf DH (2008) Degradation of misfolded protein in the cytoplasm is mediated by the ubiquitin ligase Ubr1. *FEBS Lett* 582:4143–4146.
41. Heck JW, Cheung SK, Hampton RY (2010) Cytoplasmic protein quality control degradation mediated by parallel actions of the E3 ubiquitin ligases Ubr1 and San1. *Proc Natl Acad Sci USA* 107:1106–1111.
42. Prasad R, Kawaguchi S, Ng DT (2012) Biosynthetic mode can determine the mechanism of protein quality control. *Biochem Biophys Res Commun* 425:689–695.
43. Nillegoda NB, et al. (2010) Ubr1 and Ubr2 function in a quality control pathway for degradation of unfolded cytosolic proteins. *Mol Biol Cell* 21:2102–2116.
44. Shemorry A, Hwang CS, Varshavsky A (2013) Control of protein quality and stoichiometries by N-terminal acetylation and the N-end rule pathway. *Mol Cell* 50:540–551.
45. Aksnes H, Drazic A, Marie M, Arnesen T (2016) First things first: Vital protein marks by N-terminal acetyltransferases. *Trends Biochem Sci* 41:746–760.
46. Dörfel MJ, Lyon GJ (2015) The biological functions of Naa10 - From amino-terminal acetylation to human disease. *Gene* 567:103–131.
47. Scott DC, Monda JK, Bennett EJ, Harper JW, Schulman BA (2011) N-terminal acetylation acts as an avidity enhancer within an interconnected multiprotein complex. *Science* 334:674–678.
48. Becker T, Weber K, Johnsson N (1990) Protein-protein recognition via short amphiphilic helices; a mutational analysis of the binding site of annexin II for p11. *EMBO J* 9: 4207–4213.
49. Monda JK, et al. (2013) Structural conservation of distinctive N-terminal acetylation-dependent interactions across a family of mammalian NEDD8 ligation enzymes. *Structure* 21:42–53.
50. Zhang Z, Kulkarni K, Hanrahan SJ, Thompson AJ, Barford D (2010) The APC/C subunit Cdc16/Cut9 is a contiguous tetratricopeptide repeat superhelix with a homo-dimer interface similar to Cdc27. *EMBO J* 29:3733–3744.
51. Menssen R, et al. (2012) Exploring the topology of the Gid complex, the E3 ubiquitin ligase involved in catabolite-induced degradation of gluconeogenic enzymes. *J Biol Chem* 287:25602–25614.
52. Hung G-C, Brown CR, Wolfe AB, Liu J, Chiang H-L (2004) Degradation of the gluconeogenic enzymes fructose-1,6-bisphosphatase and malate dehydrogenase is mediated by distinct proteolytic pathways and signaling events. *J Biol Chem* 279: 49138–49150.
53. Kötter P, Weigand JE, Meyer B, Entian K-D, Suess B (2009) A fast and efficient translational control system for conditional expression of yeast genes. *Nucleic Acids Res* 37:e120.
54. Tapia-Alveal C, Calonge TM, O'Connell MJ (2009) Regulation of Chk1. *Cell Div* 4:8.
55. Mandal AK, et al. (2007) Cdc37 has distinct roles in protein kinase quality control that protect nascent chains from degradation and promote posttranslational maturation. *J Cell Biol* 176:319–328.
56. McClellan AJ, et al. (2007) Diverse cellular functions of the Hsp90 molecular chaperone uncovered using systems approaches. *Cell* 131:121–135.
57. Schrader EK, Harstad KG, Matouschek A (2009) Targeting proteins for degradation. *Nat Chem Biol* 5:815–822.
58. McShane E, et al. (2016) Kinetic analysis of protein stability reveals age-dependent degradation. *Cell* 167:803–815.
59. Duttler S, Pechmann S, Frydman J (2013) Principles of cotranslational ubiquitination and quality control at the ribosome. *Mol Cell* 50:379–393.
60. Hwang CS, Varshavsky A (2008) Regulation of peptide import through phosphorylation of Ubr1, the ubiquitin ligase of the N-end rule pathway. *Proc Natl Acad Sci USA* 105:19188–19193.
61. Vidal M, Fields S (2014) The yeast two-hybrid assay: Still finding connections after 25 years. *Nat Methods* 11:1203–1206.
62. Johnsson N, Varshavsky A (1994) Split ubiquitin as a sensor of protein interactions in vivo. *Proc Natl Acad Sci USA* 91:10340–10344.
63. Dünkler A, Müller J, Johnsson N (2012) Detecting protein-protein interactions with the split-ubiquitin sensor. *Methods Mol Biol* 786:115–130.
64. Holmes WM, Mannakee BK, Gutenkunst RN, Serio TR (2014) Loss of amino-terminal acetylation suppresses a prion phenotype by modulating global protein folding. *Nat Commun* 5:4383.
65. Yi CH, et al. (2011) Metabolic regulation of protein N-alpha-acetylation by Bcl-xL promotes cell survival. *Cell* 146:607–620.
66. Linster E, et al. (2015) Downregulation of N-terminal acetylation triggers ABA-mediated drought responses in Arabidopsis. *Nat Commun* 6:7640.